Arch. Metall. Mater. **70** (2025), 2, 625-632

DOI: https://doi.org/10.24425/amm.2025.153463

MANH TIEN NGUYEN[1*], TRUONG AN NGUYEN[1]

MICROSTRUCTURE AND MICROHARDNESS OF AA6061 ALUMINUM ALLOY FORMED BY CYCLIC EXPANSION-EXTRUSION PROCESS: NUMERICAL SIMULATION AND EXPERIMENTAL EVALUATION

This paper reports numerical simulation and experimental evaluation of the cyclic expansion-extrusion (CEE) process of AA6061 aluminum alloy. Commercial software Deform 2D was used to simulate the deformation process. The material model is set up for the simulation problem by tensile tests. Simulation results are exploited including stress-strain field during the CEE process. They clearly explain the mechanism of severe plastic deformation (SPD) of the CEE method, one of the methods to create ultrafine grains (UFGs) in microstructures for the studied alloy. Tensile and CEE tests were performed at room temperature. The corresponding experimental results also show changes in the microstructure and microhardness of the test specimens. After the cycles of the CEE process, the average microhardness of the deformed specimens increased by approximately 150% compared to the initial microhardness. The UFGs in microstructures were obtained after 4 CEE cycles. The average grain size in the microstructure has been achieved at about 5÷6 μm from the initial value of 100 μm. The results of the paper show the applicability of the CEE method in the fabrication of UFGs materials for subsequent special forming processes.

Keywords: Cyclic expansion-extrusion; UFGs; microstructure; AA6061 aluminum alloy

1. Introduction

Aluminum alloys have better synthetic mechanical properties than pure aluminum: high specific strength, good corrosion resistance, lightweight, easy fabrication, and cheaper. Important applications of aluminum alloys to meet increasingly high technical requirements in the aerospace, automotive, and military industries... [1-3]. However, the deformability of aluminum alloy in the supplied state is relatively limited. Under tensile test conditions at room temperature, the relative elongation of the tensile specimens is only about 10 to 15%. Some aluminum alloys have the same strength as some steel. The relative elongation of even tensile specimens is only 5 to 8%. Therefore, to be able to deform aluminum alloys with a greater degree of deformation, it is necessary to prepare for the microstructural and mechanical properties of these alloys and to apply special forming technologies [4,5].

Severe plastic deformation (SPD) processes are generalized as metal forming processes with a very high degree of plastic strain to produce UFGs materials [6,7]. The UFGs materials are used to make lightweight and high-strength products using new forming technologies such as superplastic forming (SPF). This process allows plastic deformation with a large degree of metal or alloy under certain conditions of microstructure, temperature, and strain rate under the effect of stress of small value and dependent on strain rate [8-10]. Thus, the preparation of microstructural and mechanical properties for aluminum alloys is an important condition to enhance the plastic deformation ability of them by SPF. Therefore, the SPD methods are mentioned and studied in both simulation and experimental evaluation. Commonly performed SPD processes today include equal channel angular pressing (ECAP), high pressure torsion (HPT), multidirectional forging (MDF), and cyclic extrusion compression (CEC)... [11-15].

Chang et al. [12] reported on the ECAP process to produce AlMgSi alloy with UFGs in microstructures. The ECAP cycle was performed with four presses with an intermediate annealing between the two presses. Research results show that the studied alloy achieves increased strength along with a significant reduction in microstructures. The UFGs in microstructures were obtained after four presses. Not only that, a dislocation with high density is observed in the crystalline grains. These are the important properties of the studied alloy for the subsequent deformation processes. The disadvantage of this SPD method is the high press pressure associated with high-capacity equipment. In addition, the loss in volume of pressed samples is relatively significant after each pressing. Therefore, the application of this method

[1] LE QUY DON TECHNICAL UNIVERSITY, FACULTY OF MECHANICAL ENGINEERING, HA NOI, VIET NAM

* Corresponding author: manhtiennguyen84@lqdtu.edu.vn

has certain limitations. Z Horita et al. [13] has experimentally evaluated the effect of HPT on the mechanical properties and microstructure of Al-3 wt.% Mg-0.2 wt.% Sc alloy. Significant grain refinement is obtained after the HPT process. The average grain size in the microstructure of the studied alloy is approximately 150 nm. This method is effectively applied to brittle and high-strength alloys. The increase in microhardness near the edges of the deformed alloy disc is much higher than that of the original workpiece. However, unevenness in the radial stiffness of the workpiece after HPT was also reported. This result has a significant influence on the quality of embryos provided for the subsequent forming processes. Nguyen et al. [14] have also used a SPD technique to create UFGs in microstructures for Ti5Al3Mo1.5 V alloy because of its outstanding applications in the aerospace industry. A MDF cycle is performed by rotating the workpiece in all three directions at high temperatures. A useful contribution of the study is the evaluation of the superplastic properties of Ti5Al3Mo1.5 V alloy after SPD. Excellent deformation of single tensile samples is obtained at more than 1000%. However, in the process of making MDF, the intermediate steps often have to be reprocessed, so it takes time in the experimental process. Moreover, the MDF process will lead to a sudden increase in forging force, making it difficult to choose testing equipment. G. El-Garhy et al. [15] presented research results related to the application of the CEC method to create materials with outstanding properties in terms of microstructure, physical, and mechanics. After the CEC processes it is possible to reduce the average grain size of the crystal grains, increase the hardness and increase the anti-wear properties of the alloy. The key factor that makes this method possible is the use of back pressure to form the workpiece along the die cavity in the second step [16]. The results of the test samples through the steps of the CEC process retain the same form and size. This is a distinct advantage compared to the ECAP and HPT methods. However, this is the factor that causes significant difficulties for this method in the process parameter control and tool design. On the basis of analyzing the advantages and disadvantages of SPD techniques for the production of bulk workpieces, many recent studies refer to a simpler method. The proposed cyclic expansion-extrusion (CEE) method differs from the CEC method in that the cross-section of the die cavity used for the extrusion of the workpiece is expanded to the cavity containing the initial workpiece. The pressure required to deform the workpiece to fill the cavity extension is essentially equivalent to the back pressure [17-19]. The deformation die for the CEE method is much simpler than that of similar methods.

Based on the mentioned arguments, the paper focuses on numerical simulation and experimental evaluation of the CEE process. Commercial software Deform 2D was used to simulate the deformation process. First, tensile tests are performed to build a behavior model of the studied alloy for numerical simulation calculations. The stress-strain field of the deformed workpiece is investigated to confirm the deformability of the workpiece using the CEE method. Experimental results were evaluated through the microstructure and microhardness of the test specimens after CEE cycles. The results of the paper show the applicability of the CEE method in manufacturing UFG materials for subsequent forming technologies of AA6061 aluminum alloy.

2. Materials and methods

2.1. Materials and material model for deformation

The aluminum alloy AA6061 is used in simulation and experiments. The chemical composition of the analyzed AA6061 alloy is shown in TABLE 1 expressed in weight percent (wt.%).

TABLE 1

Chemical composition of the analyzed AA6061 alloy

Mg	Si	Cu	Fe	Mn	Cr	Zn	Ti	Al
1.004	0.59	0.26	0.371	0.097	0.141	0.066	0.037	balanced

A model of the hardening plastic material of P. Ludviga is built for the deformation process of aluminum alloy AA6061. The stress-strain rate relationship can be described by the phenomenological model presented in Eq. (1).

$$\sigma = K\varepsilon^n \tag{1}$$

where σ is the effective flow stress (MPa), K is is the strain hardening coefficient (MPa), ε is the effective strain, n is the strain hardening exponent.

The coefficients of the material model are determined through tensile tests. Tensile specimens are cylindrical as standard (ISO 6892-1:2009). The length and diameter of the working part of the tensile specimens are 50 mm and 15 mm, respectively (Fig. 1b). The tensile specimens are clamped by the series 647 hydraulic wedge grips (Fig. 1a) [20]. During the test, The tensile samples were deformed at a nominal strain rate of 10^{-3} s^{-1}. The MTS 634.12E-24 extensometer was used to analyze the strain data obtained during the test and report the test results. Engineering stress-strain curves are determined for the deformed tests shown in Fig. 1c. Next, the true stress-strain curve is determined based on data from the engineering stress-strain curve. Engineering strain is not a satisfactory measure of strain because it is based on the original gauge length. From the values of true stress and true strain, according to [21], the coefficients of the hardening plastic material model of AA6061 alloy during the cold forming process can be determined. The coefficients K and n are 202 MPa and 0.175, respectively.

2.2. The CEE method

The CEE method can accumulate strain on a workpiece without changing its shape. CEE combines both upsetting and extrusion processes, the schematic diagram of this method is shown in Fig. 2. At stage 1, the workpiece is placed in the die, and its position limit is set by the fixed blocking punch (Fig. 2a).

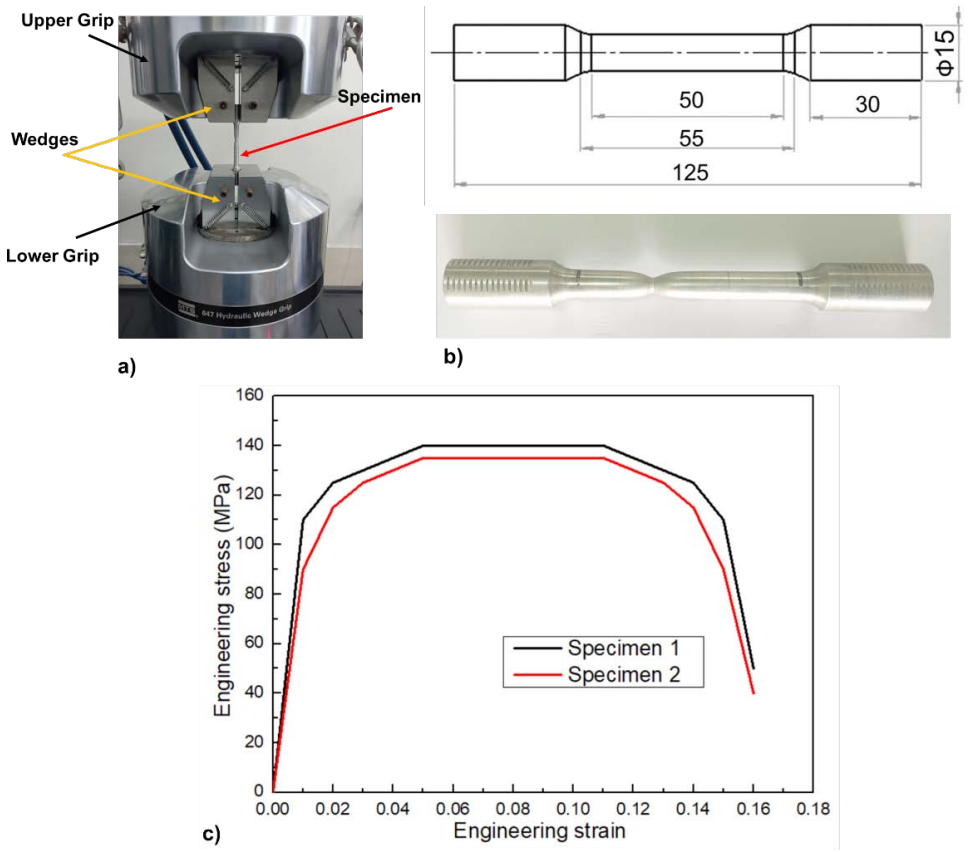

Fig. 1. The tensile test device (a), specimen and fractured specimen (b), and engineering stress-strain curve (c)

The die consists of two upper and lower chambers with the same diameter d_0. These two chambers are connected through a large cavity with a diameter $d_m (d_m > d_0)$. The pressing process is carried out by the punches with the punch stroke in the die cavity is the same. The primary punch moves down and deforms the initial samples, the samples fill the expanded die cavity. The blocking punch will ensure that the workpiece does not go beyond the neckline down (Fig. 2b). Stage 1 is performed only once in the entire CEE process. Stages 2 and 3 constitute one CEE cycle. In stage 2, the punch will continue to descend to the edge of the bulge cavity (Fig. 2c) while the blocking punch is removed to allow the workpiece to flow downwards (Fig. 2d). Next, the die will be removed from the equipment table to rotate 180 degrees, then the punch will move down to deform the workpiece (Fig. 2e), the workpiece will move down (Fig. 2f). The next cycles will be performed according to the steps of stage 2 and

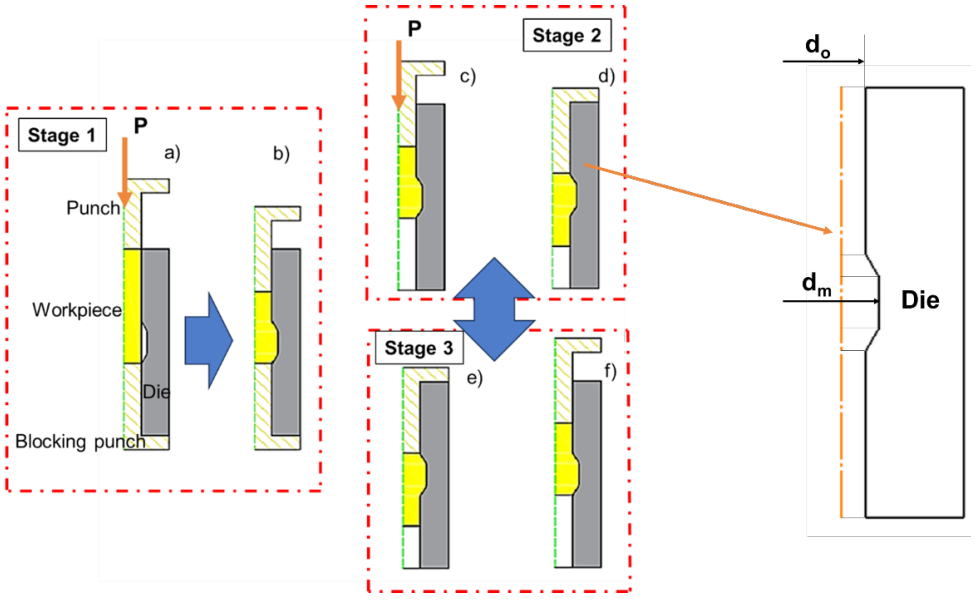

Fig. 2. Diagram of the stages of the CEE method

stage 3. Thus, the metal flow is continuously transferred from the upper cavity to the lower cavity.

The degree of strain in the CEE process is calculated similarly to the CEC method, according to Eq. (2) [18]:

$$\varepsilon = 4n \ln \frac{d_0}{d_m} \tag{2}$$

where d_0 is the die small cavity diameter approximately equal to the initial workpiece diameter, d_m is the expanded cavity diameter, and n is the number of CEE cycles.

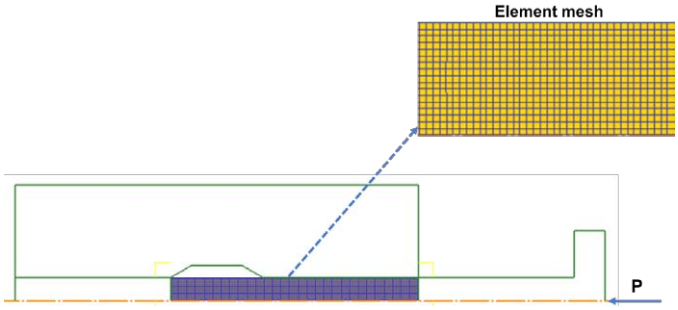

Fig. 3. The geometry model of workpiece and die

2.3. Numerical simulation of deformation processes with CEE method

Simulation of the CEE process is done on Deform-2D V11.2 software, which is an industrial software widely used in the field of metal forming. The geometry model of the CEE process is built on the software and is shown in Fig. 3a. The initial billet is cylindrical with a diameter of 15 mm and a height of 80 mm. The die small cavity diameter of 15 mm and the expanded cavity diameter of 23 mm. The material model used in simulations for AA6061 alloy is shown in Eq. (1) (Fig. 3b). For the initial meshes, the number of mesh elements to be constructed is 4000 elements. Die and punch are considered to be absolutely rigid to practice in analyzing the deformation of the workpiece after the CEE process. The CEE processes are carried out at room temperature. The pressing speed has a negligible effect on the grain size formed by the CEE process, but recovery is easier when pressing at a lower speed, it is easier to produce balanced tissue microstructures. Therefore, the pressing speed of the punch selected in Deform 2D software is 10 mm/s. The coefficient of contact friction between the workpiece and the tools is set to 0.4. The numerical simulation problems on Deform 2D software are performed for 1 to 4 CEE cycles. The results investigated after the simulations include stress, and strain during the deformation process.

2.4. Experimental process

The initial cylindrical samples with dimensions of 15 mm (diameter) × 80 mm (height) were used for the experimental process. Device system used for experiments at the laboratory of the Department of Metal Forming, Faculty of Mechanical Engineering, Le Quy Don Technical University. The LH120/13 Nabthem induction furnace is used for annealing the initial workpiece at 425°C for three hours [15]. Next, the CEE process is performed from 1 to 4 cycles. The YH32 hydraulic press with a maximum nominal force of 100 tons is used for deform CEE cycles. The force of each press is determined through the pressure value applied to the hydraulic cylinder spindle displayed on the pressure gauges. Deformation dies and hydraulic press and deformed specimens are shown in Fig. 4.

The initial and post-CEE samples were examined for Vickers microhardness (Hv). Microhardness measurements are carried out at five equally spaced points on the axial cross-section of the specimens in two directions: the horizontal direction and the vertical direction relative to the axis of symmetry of the specimens. The Mitutoyo Hardness test machine is used for the microhardness testing process according to ASTM E384-17 standard. Finally, the microscopic examination was also carried out on both horizontal and vertical sections. Specimens polished and etched according to the Keller method consisted

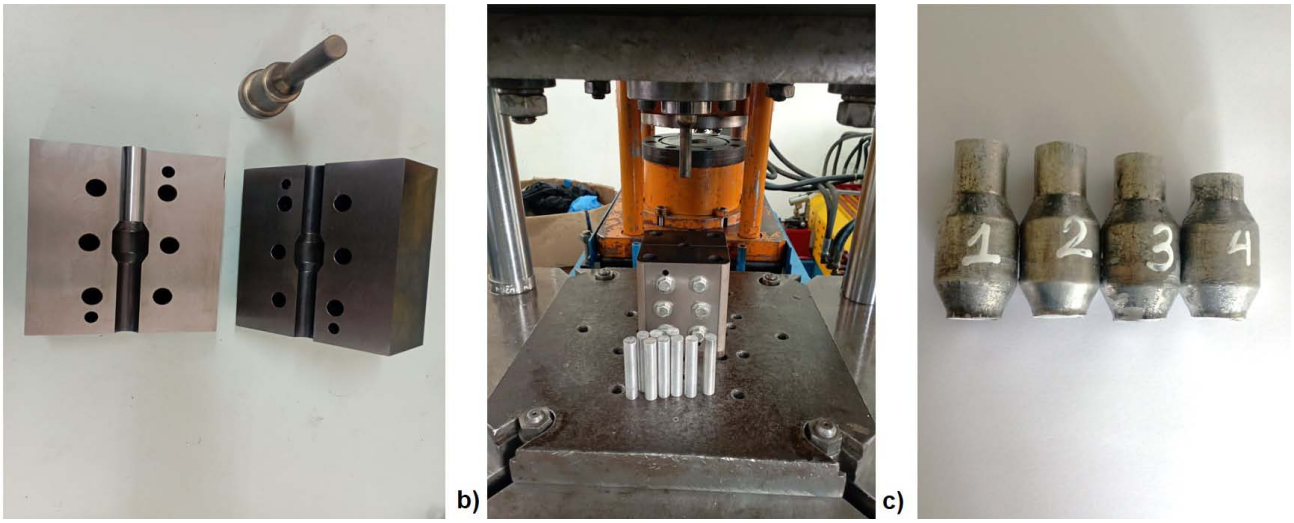

Fig. 4. Deformation dies (a) and hydraulic press (b) and deformed specimens (c)

of a solution mixture of 95 mL H_2O, 2.5 mL of HNO_3, 1.5 mL HCl, and 1.0 mL HF. The Axio Observer A2M Carl Zeiss optical microscope is used for microstructure examination. The Jeffris method is applied to measure the average grain size through the captured microstructure images.

3. Results and discussion

3.1. Numerical simulation results

The change in the stress field of the specimens during the CEE process was evaluated over the cavity filling phase (stage 1) and the CEE cycles (stage 2 and stage 3). The cavity filling phase when the primary punch begins to touch the workpiece deforms and fills the expanded die cavity. The increased effective stress reaches the yield strength of the aluminum alloy AA6061. The effective stress of the specimen after cycles is shown in Fig. 5.

The effective stress in the specimens in the expanded die is mostly above the yield strength of the alloy, only the part in contact with the punch has less stress. The metal at the necks is subjected to great stress due to strong hardening. The maximum effective stress after the 1 cycle increases sharply to 270 MPa. This stress value of the subsequent cycles is almost constant and it is approximately equal to 250 MPa. The stress field distribution after CEE cycles is different from that of the CEC method. The stress distribution in the deformed specimens of the CEC process will be more uniform due to the back pressure created by the auxiliary punch during the deformation process. However, these simulation results indicate that it is the increased effective stress in the neck regions between the expanded die cavity and the small die cavity that acts as the back pressure. Based on the effective stress distribution, the strain in the specimens after CEE cycles will be more uniform. The increased degree of accumulated strain through CEE cycles is one of the conditions for creating the UFGs in microstructures according to the deformation mechanism of SPD techniques [18].

The maximum effective strain value of the specimens over the CEE cycles is investigated and shown in Fig. 6. Through the evaluation of the strain field with a different number of cycles

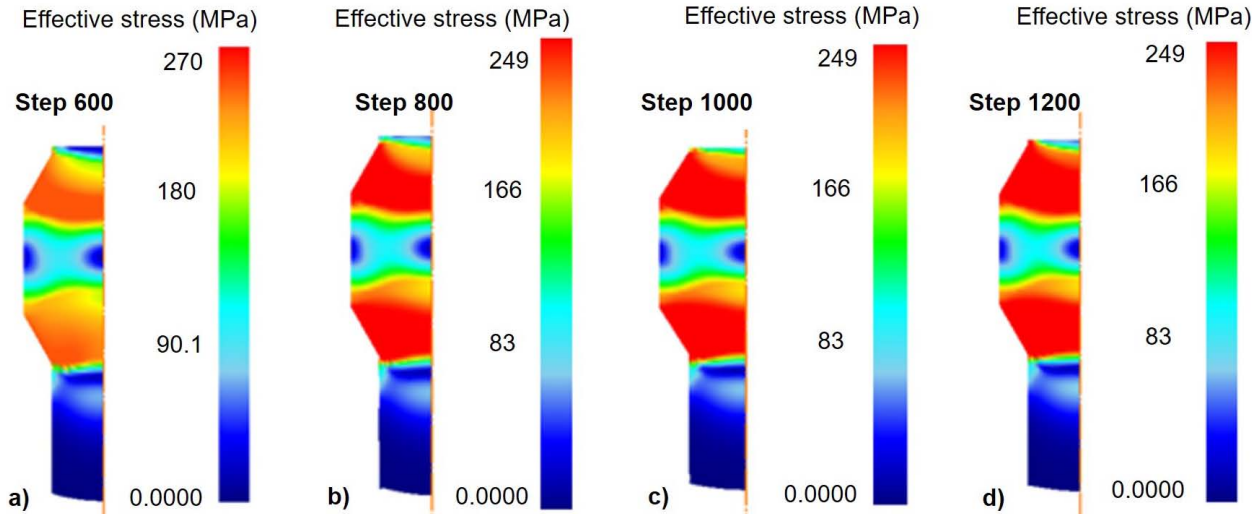

Fig. 5. The effective stress of the specimen after CEE cycles: a) 1 cycle, b) 2 cycles, c) 3 cycles, d) 4 cycles

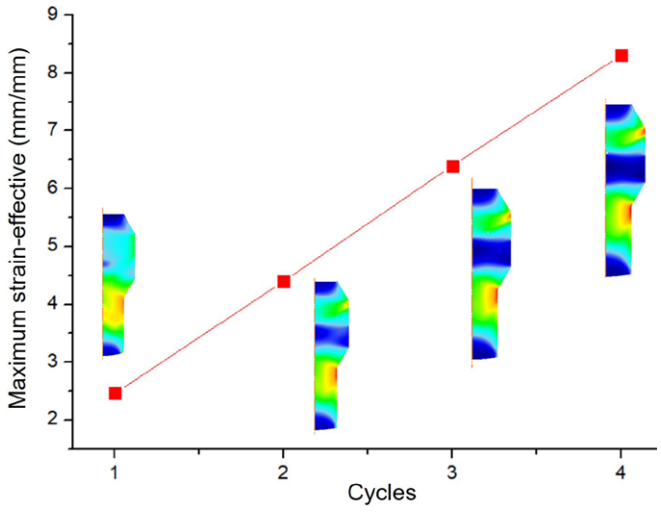

Fig. 6. The effective strain of the specimen after CEE cycles

through CEE, it is found that with the increase in the number of cycles (the degree of accumulated strain increases), the alloy deforms better. The maximum effective strain of the deformed specimens increased from 1.12 mm/mm to 8.31 mm/mm, corresponding from 1 cycle to 4 cycles. Thus, increasing the degree of accumulated strain leads to better plastic deformation ability of the specimens. This must also take into account the role of the neck parts of the CEE die. The deformation resistance created by them helps other parts of the specimens to be deformed better.

3.2. Experimental results

Initial and post-CEE specimens were cut in the axial section. The cross-section is smoothed for microhardness measurements. The microhardness is determined at measuring points from the

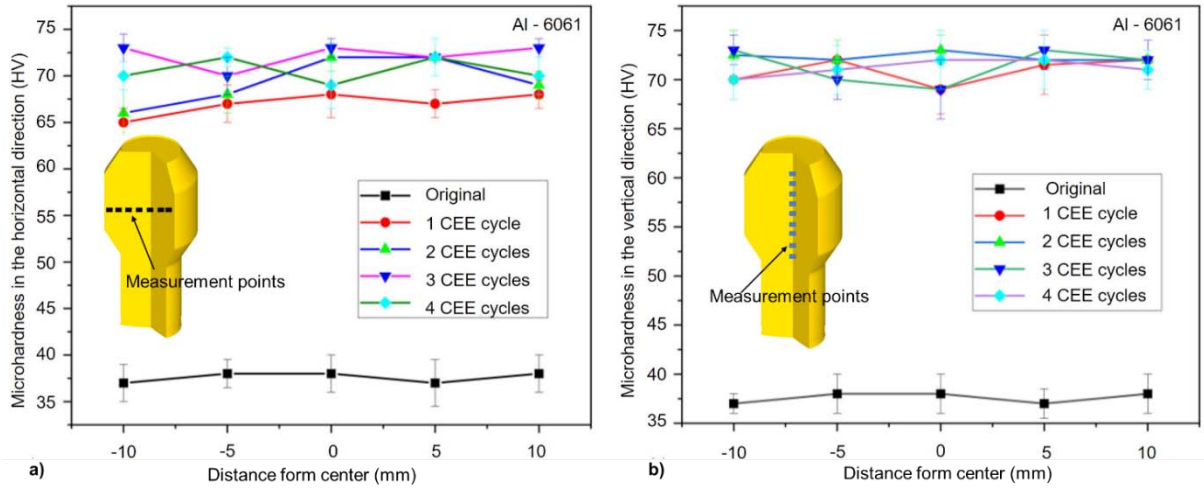

Fig. 7. The microhardness in the horizontal direction (a) and the vertical direction (b) relative to the axis of symmetry of the specimens, for 1 or 4 CEE cycles and original specimens

center of the specimen surface in the horizontal and vertical directions relative to the axis of symmetry of the specimens, spaced by 5 mm. Microhardness measurement results are shown in Fig. 8a and Fig. 8b for the horizontal and vertical directions, respectively.

The measured microhardness after 1 CEE cycle in the two directions mentioned above is significant heterogeneity, the microhardness at the peripheral surface shows a significantly higher than the microhardness at the center of the deformed specimens. This result is similar to the conventional extrusion process due to the effects of hardening and contact friction of the peripheral surface and the deformation tool. However, the microhardness values are relatively uniform between the measuring points in both the vertical direction and horizontal direction to the symmetry axis of the next CEE cycles. Thus, it can be estimated that the microhardness uniformity in a deformed sample increases with an increasing number of CEE cycles. This result is explained by the increase in the amount of accumulated strain over the CEE cycles, leading to the saturation of the microhardness value of the aluminum alloy AA6061 [6].

As shown in Fig. 7, it was found that the average microhardness of the deformed specimens increased sharply after 1 CEE cycle from 40 Hv to 65 Hv. Thereafter, there was a negligible increase after the 2 CEE cycle. It is particularly noticeable that in subsequent cycles, the microhardness of the samples hardly changes (Hv ≈ 70). This result is explained by the hardening after 1 CEE cycle, so the average microhardness of the deformed specimens increases significantly. The degree of accumulated strain over subsequent CEE cycles results in a small change in the average microhardness. This is one of the important characteristics of SPD methods that affect the mechanical properties of materials [6,7].

Fig. 8(a-d) and Fig. 8(f-i) show the microstructures of the CEEed specimens in the horizontal and vertical direction relative to the axis of symmetry of the specimens. The average grain size of the deformed specimens in the horizontal direction is equal to 11.3 ± 0.05 μm, 9.3 ± 0.03 μm, 7.0 ± 0.02 μm, 5.3 ± 0.01 for the 1 cycle, 2 cycles, 3 cycles, 4 cycles, respectively. The average grain size of the deformed specimens in the vertical direction is equal to 13 ± 0.05 μm, 9.8 ± 0.03 μm, 7.2 ± 0.02 μm, 5.5 ± 0.01 for the 1 cycle, 2 cycles, 3 cycles, 4 cycles, respectively. Meanwhile, the initial average grain size of the specimens after annealing was 100 μm.

The experimental results showed a significant reduction in average grain size after 4 cycles of the CEE processes. During the first cycle of the CEE process, the elongation of the crystals was observed in both the horizontal and the vertical directions. This change corresponds to the process of filling the die cavity by the upsetting method. Moreover, at this time, the degree of accumulated strain is not large enough to separate the crystal grains. In the subsequent CEE cycles, we find that with the increase of the degree of accumulated strain, the crystal grains tend to split to form grains with smaller average grain sizes. Then, due to the formation of larger stress zones at the die neck positions, the deformed particles mainly in the cavity expand with a greater degree of strain. The crystal grains will be separated in a larger number to create ultrafine grains (UFGs) in microstructures for the studied alloy [6,14]. The results also show that after 4 CEE cycles, the average grain sizes of the deformed specimens are similar in both the horizontal and the vertical directions. It can be asserted that the CEE process allows to achievement of UFG in the microstructure of the studied alloy.

4. Conclusions

In this study, an aluminum alloy AA6061 in the cast state is deformed to a large degree of cumulative strain with 4 cycles according to the CEE method. The microhardness and microstructures were investigated experimentally. Numerical simulation is applied to compare with the experimental process. The main results achieved include:

(1) The simulation results show that the stress distribution in the deformed specimens is not uniform. The effective stress

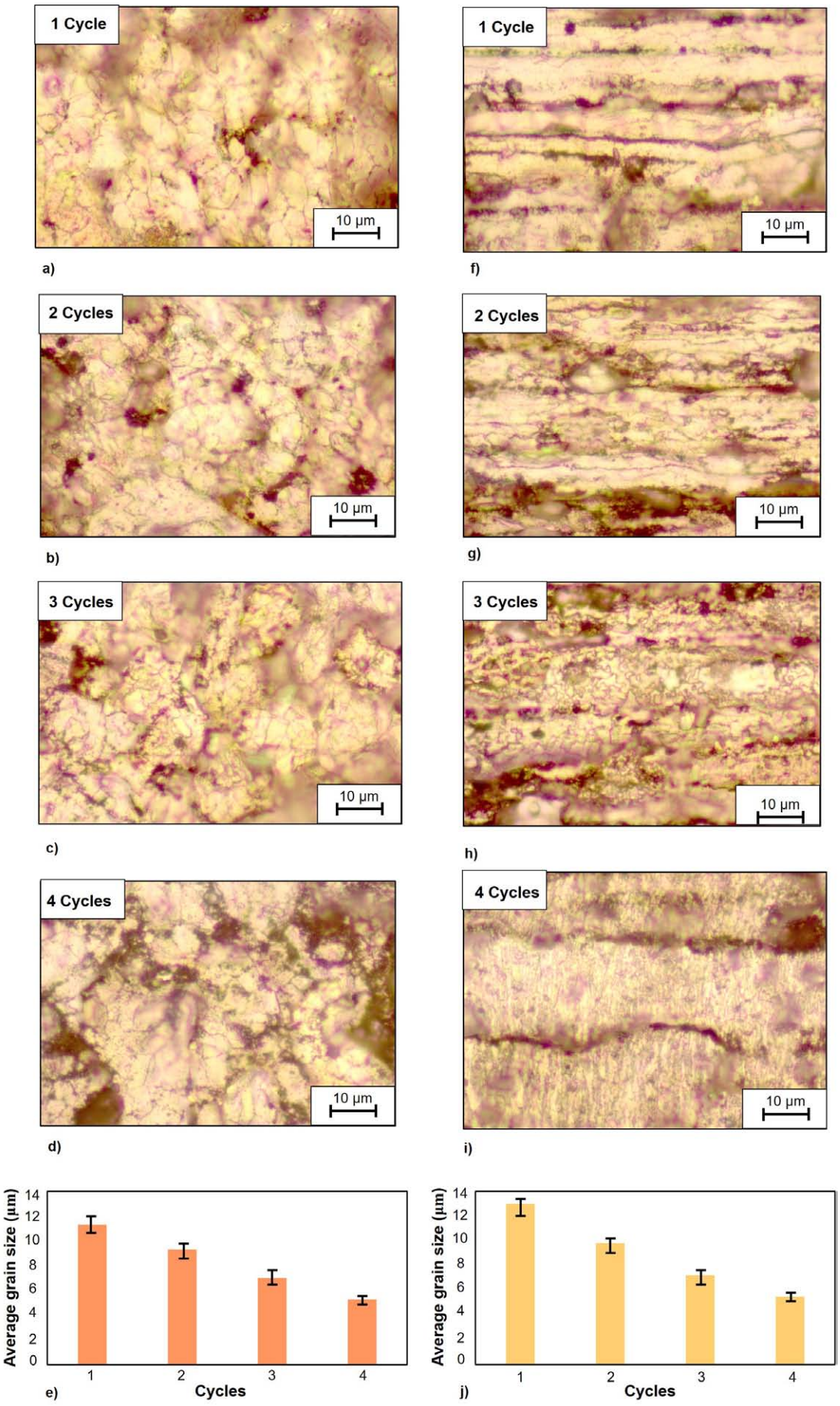

Fig. 8. The microstructures and average grain size of the deformed specimens after CEE cycles in the horizontal direction (a, b, c, d, e) and the vertical direction (f, g, h, i, j)

has a large value at the neck between the expansion and the small part of the die cavity. This effective stress is equivalent to the back pressure performed in the CEC method. This allows for increased deformation of the specimens and it has an important effect on the mechanical properties and microstructures of the studied alloy.

(2) The value of the microhardness increased sharply after 1 CEE cycle from 40 Hv to approximately 65 Hv. In subsequent cycles, the microhardness of the samples hardly changes (Hv ≈ 70). This result is explained by the hardening after 1 CEE cycle, so the average microhardness of the deformed specimens increases significantly. The accumulated strain over subsequent CEE cycles results in a small change in the average microhardness.

(3) The UFGs in microstructures were obtained after 4 CEE cycles. The average grain size in the microstructure has been achieved at about 5÷6 μm. This result shows that the aluminum alloy AA6061 is deformed by the CEE method and meets the conditions of microstructure for SPF.

REFERENCES

[1] W. Zhou, Z. Shao, J. Yu, J. Lin, Advances and Trends in Forming Curved Extrusion Profiles. Materials **2021** (14), 1603 (2021). DOI: https://doi.org/10.3390/ma14071603

[2] R.J. Bhatt, Advanced Approaches in Superplastic Forming-A Case Study. J. Basic Appl. Eng. Res. **1** (2), 57-64 (2014).

[3] X. Zhang, Y. Chen, J. Hu, Recent Advances in the Development of Aerospace Materials. Prog. Aerosp. Sci. **97**, 22-34 (2018). DOI: https://doi.org/10.1016/j.paerosci.2018.01.001

[4] N.E. Prasad, A.A. Gokhale, R.J.H. Wanhill, Aluminum-Lithium Alloys: Processing, Properties, and Applications, Oxford: Elsevier, 2014.

[5] N. Eswara Prasad, Amol Gokhale, R.J.H Wanhill, Aluminum--Lithium Alloys. Processing, Properties, and Applications, Butterworth-Heinemann: Elsevier, 2014.

[6] A. Azushima, et al., Severe Plastic Deformation (SPD) Process for Metals. CIRP Annals **57** (2), 716-735 (2008). DOI: https://doi.org/10.1016/j.cirp.2008.09.005

[7] R.Z. Valiev, Recent Developments of SPD Processing for Fabrication of Bulk Nanostructured Materials. 4th International Conference on Processing and Manufacturing of Advanced **426** (4), 237-244 (2002). DOI: https://doi.org/10.1002/9781118804537.ch37

[8] M.T. Nguyen, T.A. Nguyen, D.H. Tran, V.T. Le, Optimization of Superplastic Forming Process of AA7075 Alloy for the Best Wall Thickness Distribution. Adv. Technol. Innov. **6** (4), 251-261 (2021). DOI: https://doi.org/10.46604/aiti.2021.7835

[9] Fadi K. Abu-Farha, Marwan K. Khraisheh, An Integrated Approach to the Superplastic Forming of Lightweight Alloys: towards Sustainable Manufacturing. Int. J. Sustain. Manuf. **1** (1/2), 18-40 (2008). DOI: https://doi.org/10.1504/IJSM.2008.019225

[10] W. Zhou, J. Lin, D.S. Balint, T.A. Dean, Clarification of the Effect of Temperature and Strain Rate on Workpiece Deformation Behaviour in Metal Forming Processes. J. Mach. Tools Manuf. **171**, 103815 (2021). DOI: https://doi.org/10.1016/j.ijmachtools.2021.103815

[11] W. Zhou, J. Yu, J. Lin, T.A. Dean, Manufacturing a Curved Profile with Fine Grains and High Strength by Differential Velocity Sideways Extrusion. J. Mach. Tools Manuf. **140**, 77-88 (2019). DOI: https://doi.org/10.1016/j.ijmachtools.2019.03.002

[12] J.Y. Chang, A. Shan, Microstructure and Mechanical Properties of AlMgSi Alloys after Equal Channel Angular Pressing at Room Temperature. Mater. Sci. Eng. **347** (1-2), 165-170 (2003). DOI: https://doi.org/10.1016/S0921-5093(02)00577-4

[13] Zenji Horita, Terence G. Langdon, Microstructures and Microhardness of an Aluminum Alloy and Pure Copper after Processing by High-pressure Porsion. Mater. Sci. Eng. A. **410**, 422-425 (2005). DOI: https://doi.org/10.1016/j.msea.2005.08.133

[14] M.T. Nguyen, V.T. Le, M.H. Le, T.A. Nguyen, Superplastic Properties in a Ti5Al3Mo1.5 V Titan Alloy Processed by Multidirectional Forging Process. Mater. Lett. **307**, 131004 (2022). DOI: https://doi.org/10.1016/j.matlet.2021.131004

[15] G. El-Garhy, N. El Mahallawy, M.K. Shoukry, Effect of Grain Refining by Cyclic Extrusion Compression (CEC) of Al-6061 and Al-6061/SiC on Wear Behavior. J. Mater. Res. Technol. **12**, 1886-1897(2021). DOI: https://doi.org/10.1016/j.jmrt.2021.03.114

[16] M. Richert, H. Petryk, S.S tupkiewicz, Grain Refinement in AlMgSi Alloy During Cyclic Extrusion-Compression: Experiment And Modelling. Arch. Metall. Mater. **52** (1), 1-11 (2007).

[17] H. Fan, Z. Yan, Z. Zhang, Q. Wang, Effects of Cyclic Expansion-Extrusion with an Asymmetrical Extrusion Cavity (CEE-AEC) on the Microstructure and Texture Evolution of Mg-13Gd-4Y-2Zn-0.5Zr Alloys. Mater Technol. **54** (4), 495-501 (2020). DOI: https://doi.org/10.17222/mit.2019.251

[18] N. Pardis, B. Talebanpour, R. Ebrahimi, S. Zomorodian, Cyclic Expansion-Extrusion (CEE): A Modified Counterpart of Cyclic Extrusion-Compression (CEC). Mater. Sci. Eng. A. **528** (25-26), 7537-7540 (2011). DOI: https://doi.org/10.1016/j.msea.2011.06.059

[19] Y. Xue, Z. Yang, B. Bai, Z. Zhang, Y. Du, L. Ren, Effect of Different Cyclic Expansion-Extrusion Processes on Microstructure and Mechanical Properties of AZ80 Magnesium Alloy. Adv. Mech. Eng. **9** (4), 1-8 (2017). DOI: https://doi.org/10.1177/1687814017696657

[20] Y. Peng, X. Chen, S. Peng, C. Chen, J. Li,G. Liu, Strain Rate-Dependent Constitutive and Low Stress Triaxiality Fracture Behavior Investigation of 6005 Al Alloy. Adv. Mater. Sci. Eng. **2018**, 1-14 (2018). DOI: https://doi.org/10.1155/2018/2712937

[21] Z. Marciniak, J.L. Duncan, S.J. Hu, Mechanics of Sheet Metal Forming, Butterworth-Heinemann, Oxford, 2002.